SAND98-1625C

Optical properties of InGaAsN: A new 1eV bandgap material system

E. D. Jones [†a], N. A. Modine [a], A. A. Allerman [a], I. J. Fritz [a],
S. R. Kurtz [a], A. F. Wright [a], S. T. Tozer [b], X. Wei [b]

[a]Sandia National Laboratories, P. O. Box 5800, Albuquerque, NM 87185-0601
[b]National High Magnetic Field Laboratory, Florida State University, Tallahassee, FL 32306-4005

ABSTRACT

InGaAsN is a new semiconductor alloy system with the remarkable property that the inclusion of only 2% nitrogen reduces the bandgap by more than 30%. In order to help understand the physical origin of this extreme deviation from the typically observed nearly linear dependence of alloy properties on concentration, we have investigated the pressure dependence of the excited state energies using both experimental and theoretical methods. We report measurements of the low temperature photoluminescence energy of the material for pressures between ambient and 110 kbar. We describe a simple, density-functional-theory-based approach to calculating the pressure dependence of low lying excitation energies for low concentration alloys. The theoretically predicted pressure dependence of the bandgap is in excellent agreement with the experimental data. Based on the results of our calculations, we suggest an explanation for the strongly non-linear pressure dependence of the bandgap that, surprisingly, does not involve a nitrogen impurity band. Additionally, conduction-band mass measurements, measured by three different techniques, will be described and finally, the magnetoluminescence determined pressure coefficient for the conduction-band mass is measured.

Keywords: InGaAsN, band structure, LDA, photoluminescence, pressure dependent energy gaps, conduction-band mass.

1. INTRODUCTION

The quaternary alloy system, InGaAsN, is a new material system that appears to have many exciting and important device applications. Because of a large negative bowing parameter,[1,2] the addition of small amount of nitrogen to the 1.4 eV bandgap energy GaAs system *lowers the energy*! With the bandgap energy of GaN ~ 3.5 eV, normally, one would expect that the GaAsN alloy bandgap energy would increase with nitrogen content. Besides also lowering the bandgap energy, adding indium to GaAsN strain compensates the effect of nitrogen, resulting in a material system with bandgap energies ~ 1eV and lattice matched to GaAs! The InGaAsN, alloy system has been identified as a key candidate material for long wavelength laser systems.[3-5] and high-efficiency multi-junction solar cells.[6,7] While light emitting diodes (LED) based on InGaAsN have not yet been reported, this could be an ideal system to provide infrared wavelength LED's. Lattice matching allows the design of optoelectronic devices without the inherent problems found in strained systems. Of prime importance is the role of the nitrogen isoelectronic atom: (1) What is the origin of the large bandgap reduction? (2) Are the states extended (band-like) or localized (impurity-like)? In order to answer these questions, a better understanding of the electronic properties of this type of alloy system is required. (3) How is the nominally light GaAs conduction-band effective mass $m_c = 0.067$ affected by the addition of nitrogen? For optimum device performance, these questions have to be addressed.

†Correspondence: MS-0601; Email: edjones@sandia.gov; Telephone 505 844 8752; Fax: 505 844 3211

DISCLAIMER

DISCLAIMER

Portions of this document may be illegible in electronic image products. Images are produced from the best available original document.

Both first-principles[8-10] and empirical[11-14] theoretical treatments for this material system have concentrated on understanding the dependence of the bandgap energy on nitrogen composition. In the first part of this paper we review previously reported[15] pressure dependent photoluminescence (PL) data together with a first principles local density approximation (LDA) calculation for the band structure and its pressure dependence. It will be shown that, while it is well known that bandgap energies calculated by the LDA method are not accurate, the predicted pressure dependence of the bandgap energy is in excellent agreement with experiment. Similar observations have been reported for silicon.[16] Because of this good agreement, the character of the states is accurately described and we also have confidence that this technique could be useful for understanding the properties of other low concentration alloy systems.

In the second part of the paper, we present conduction-band effective mass determinations using different three different experimental techniques: (1) Studying the bandgap energy dependence as a function of InGaAsN/GaAs quantum-well width. (2) Photoreflectance measurements of the ground state and excited state energies of an InGaAsN/GaAs quantum well for various quantum-well widths. (3) Magnetoluminescence measurements of the magnetic field dependence of the InGaAsN exciton diamagnetic shift in bulk epilayers. Additionally, the pressure dependence of the conduction band-mass has also been measured using the magnetoluminescence method.

2. EXPERIMENTAL

The structures were grown in a vertical flow, high speed rotating disk, EMCORE GS/3200 metalorganic chemical vapor deposition (MOCVD) reactor. The $In_xGa_{1-x}As_{1-y}N_y$ films were grown using trimethylindium (TMIn), trimethylgallium (TMG), 100% arsine and dimethylhydrazine (DMHy). Dimethylhydrazine was used as the nitrogen source since it has a lower disassociation temperature than ammonia and has a vapor pressure of approximately 110 torr at 18°C. Unintentionally doped InGaAsN was p-type. InGaAsN films for Hall and optical measurements were grown on semi-insulating GaAs orientated 2° off (100) towards <110>. Lattice matched ($\delta a / a < 8 \times 10^{-4}$) films were grown at 600°C and 60 torr using a V/III ratio of 97, a DMHy/V ratio of 0.97 and a TMIn/III ratio of 0.12. The growth rate was 10Å/s. These conditions resulted in films with an indium mole fraction of 0.07 ± 0.005 and a nitrogen mole fraction of 0.022 ± 0.003. The composition was determined by calibration growths of GaAsN and InGaAs along with double crystal x-ray diffraction measurements. The nitrogen composition of bulk films was also confirmed from elastic recoil detection measurements. A significant increase in photoluminescence intensity was observed from these films following a post-growth anneal. Ex-situ, post-growth anneals were carried out in a rapid thermal anneal system under nitrogen using a sacrificial GaAs wafer in close proximity to the InGaAsN sample.

The photoluminescence intensity was a maximum for samples annealed either at 700°C for 2 minutes or at 650°C for 30 minutes. Similar results have been reported by Rao *et.al.*[17] Transmission electron microscopy measurements indicate that the samples are random and no evidence for clustering or phase separation was observed.[18] The pressure was generated using a small BeCu piston-cylinder diamond anvil cell, 8.75-mm-diameter and 12.5-mm-height.[19] Methanol, ethanol, and water in a ratio of 16:3:1 was used for the pressure medium.[20] The shift in the fluorescence of a small chip of ruby placed in the pressurized volume was used to calibrate the pressure at 4K with an accuracy of ±0.5 kbar.[21] A single 600-μm-diameter optical fiber, butted up against one of the diamonds, brought the 1 mW of 5145-nm-wavelength laser power to the sample and also collected the PL signal from the sample. A beam splitter system was used to direct the PL signal to an optical monochromator. Depending on the bandgap energy, two liquid-nitrogen-cooled detectors were used to detect the PL signal. For low pressure regimes, where the bandgap energies were near or below 1 eV, a NORTH-COAST EO-817L Ge-detector was employed, while at higher pressures, a standard CCD array was used.

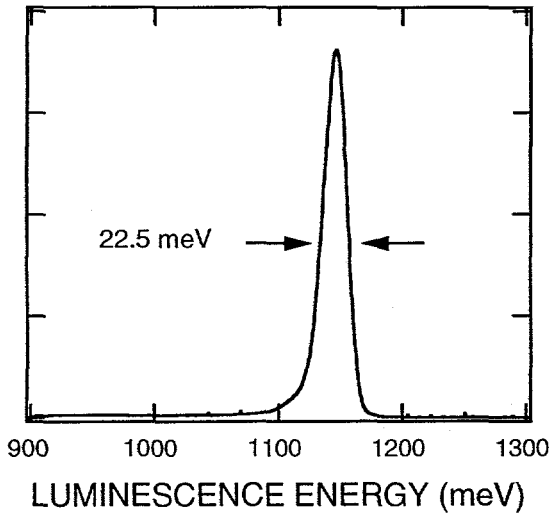

Figure 1. Low temperature (4K) PL spectrum for an annealed InGaAsN sample with 2% N. The FWHM = 22.5 meV.

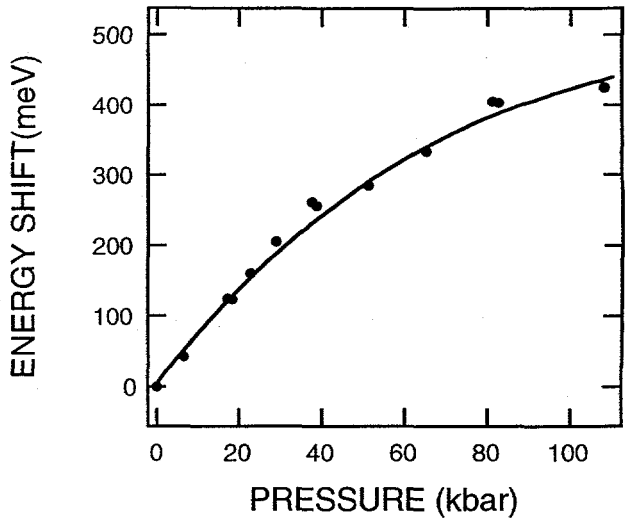

Figure 2. Experimental (dots) and theoretical (solid line) shift of the bandgap energy on pressure at 4K for 2% N in InGaAsN.

Photoreflectance spectra were obtained for a variety of MOCVD InGaAsN/GaAs MQW structures. For these experiments, the optical pump source was a blue LED having a 15 degree divergence angle and a peak emission wavelength of 470 nm (Nichia Chemical Industries part number NSPB 300A.). The LED was driven by a square-wave current source operating at 15 mA and 325 Hz. The sample reflectance was measured using a 10 W tungsten-halogen lamp followed by a 0.25-m grating monochromator in conjunction with an InGaAs photodiode detector and a lock-in amplifier.

3. DISCUSSION

A typical low temperature (4K) PL spectrum for 2% nitrogen in InGaAsN lattice matched to GaAs is shown in Fig. 1. As can be seen, the 4-K bandgap energy is near 1.15 eV, which is significantly less than the 4-K GaAs bandgap energy $E_g \approx 1515$ meV. The full-width-half-maximum (FWHM) PL linewidth is about 22.5 meV. As mentioned above, the only the PL intensity increased significantly with annealing. Other optical parameters, such as the FWHM and PL-peak energy appear to remain unaffected by our annealing process. The pressure dependence of the bandgap energy shift data, as determined from by the PL-peak energy, is shown in Fig. 2 as solid circles. The pressure data ranged between ambient and 110 kbar. The solid curve drawn through the data is discussed in the following section, however, it should be noted here that similar studies for GaAs/AlGaAs or InGaAs/GaAs quantum wells exhibit a Γ-X crossing near 40 kbar. For pressures greater than 40 kbar, the X-point becomes the conduction-band ground state and because of large non-radiative recombination paths at the X-point, the PL signal normally disappears. For the InGaAsN pressure data shown in Fig. 2, this is obviously not the case. Thus, to be able to understand the behavior of the InGaAsN system, we need information about its band structure and will be discussed in Sec 3.1. Section 3.2 presents experimental measurements and estimates for 2% nitrogen InGaAsN alloy conduction-band effective mass while Sec. 3.3 discusses the pressure dependence of the same conduction-band effective mass.

3.1 Band Structure of InGaAsN alloys

In order to model the band structure for the InGaAsN system, we used the Vienna *Ab initio* Simulation Package[22-25] (VASP) to perform first-principles electronic structure calculations based on the Kohn-Sham density functional theory with plane wave basis sets, ultrasoft pseudopotentials,[26] and the local density approximation for the exchange-correlation functional. In construction of the pseudopotentials, the Ga 3d electrons were treated as valence electrons in order to accurately represent any effects of a near resonance with the nitrogen 2s level that has been observed in GaN.[27] We modeled the InGaAsN

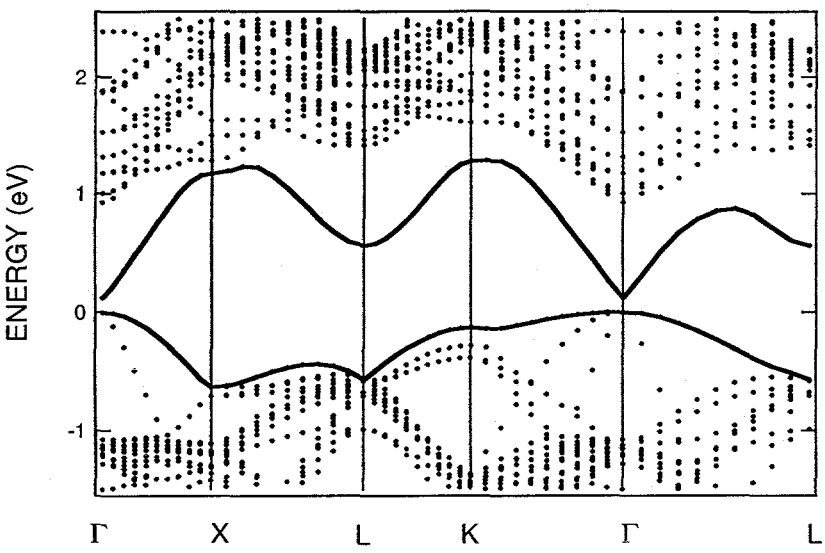

Figure 3. First principles local density approximation calculation for t3.3% nitrogen InGaAsN alloy. The solid lines, top and bottom, are respectively the conduction and valence bands.

system in the experimentally relevant concentration range using a series of supercells of the zincblende GaAs structure each with a single arsenic replaced by a nitrogen. The lattice constants of the supercells were varied to simulate the effects of pressure, and for each cell, the ionic positions were relaxed using first-principles forces until the residual forces were less than 20 meV/Å. In all cases, we found that the nitrogen atom remained in the symmetric position during relaxation. In order to compare to experimental data, which is taken as a function of pressure, an *ab initio* calculation of the system pressure was performed. We have investigated supercells with the following stoichiometries: $Ga_{32}As_{31}N$, $Ga_{64}As_{63}N$, $Ga_{108}As_{107}N$, and $Ga_{128}As_{127}N$. These cells correspond to nitrogen concentrations of 3.13, 1.56, 0.93 and 0.78%, with the nitrogen atoms ordered in simple cubic, fcc, bcc, and simple cubic lattices respectively. In contrast, the nitrogen atoms in the experimental system are believed to be nearly randomly distributed.[18] However, we found that calculated band structures of our supercells were qualitatively similar despite their differing symmetries, indicating that the nitrogen atoms interact weakly with each other at these low concentrations. Therefore, we believe that our artificially ordered supercells provide an adequate model of the near-band-gap electronic structure of the disordered experimental system. Likewise, we have ignored the presence of In in the experimental system (except for indirect effects due to the change in lattice constant, as will be discussed below). This is justified since experimental studies of InGaAs alloys indicate that the low concentration of indium found in the experimental InGaAsN system has a small effect on the electronic properties.[3,4]

Figure 3 shows a representative band structure for the 3.13% system. It should be noted that the band structure is plotted with respect to the Brillouin zone of a 64-atom cell. Since the nitrogen substitution breaks the symmetry of the underlying zincblende structure, there is no uniquely defined way to "unfold" the band structure into the Brillouin zone of the primitive 2-atom zincblende unit cell. The high symmetry points of the primitive GaAs cell fold into the Γ-point of the 64-atom cell, and therefore in the presence of a real symmetry breaking term (such as produced by nitrogen substitution), we expect interaction between the resulting levels. The valence band and the conduction band are indicated by the heavy solid line. The conduction band is well separated from the other bands throughout most of the Brillouin zone, and it is quite dispersive with a bandwidth more than 1 eV. Likewise, the bands above the conduction band show a substantial amount of dispersion, and there is no evidence of a flat impurity-like band anywhere above the conduction band. The absence of a nitrogen derived impurity-like state is supported by a decomposition of the wave-functions in terms of atomic-like orbitals, which shows that the conduction band has about 5% of its weight on the nitrogen atom, which is by far the highest fraction of any of the bands above the gap. The

calculated bandgap is only 0.12 eV, while the experimental bandgap is of order 1 eV for this concentration of nitrogen. This large error in the bandgap is a well known problem of the LDA. A central result of this paper is that despite this large error in the absolute magnitude of the bandgap, the *change* in bandgap with lattice constant is in excellent agreement with experiment (see Fig.2).

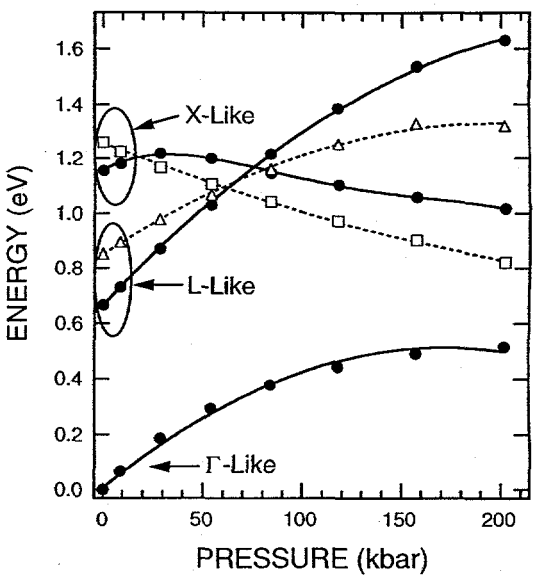

Figure 4. Theoretical pressure dependence of the conduction-band states near the bandgap energy minimum for 2% nitrogen GaAsN alloy. There are three singlets (filled circles), a doublet (open squares), and a triplet state (open triangles).

Figure 2 compares experimental data to results of our theoretical model. The agreement between theory and experiment is excellent. In order to make a meaningful comparison, some nontrivial analysis of the theoretical calculations is required. The basic principle of this analysis is to treat the lattice constant and nitrogen concentration as independent variables, while the bandgap and pressure are treated as dependent variables. The dependent variables are then shifted to remove known LDA errors. In order to obtain results applicable to the 2.0% experimental nitrogen concentration, the bandgap and the pressure are linearly interpolated between the results of 128-atom (1.56% N) and 64-atom (3.13% N) supercells for each lattice constant. Then, results obtained at the experimental lattice constant of GaAs are taken as the reference (assumed to correspond to the experimental zero of pressure), and we plot the change in bandgap against the change in pressure. This procedure compensates for two well known errors of the LDA: (1) The bandgap is severely underestimated, as discussed above. (2) The lattice constant is underestimated by about 1%. The second error may seem to be insignificant compared to the errors in LDA results for some other quantities, but it corresponds to about a 20 kbar error in pressure, which is significant on an experimental scale. Since the experimental GaAs lattice constant is used, this procedure also helps to implicitly compensate for neglecting the In, which is added to the experimental system to match the lattice constant to that of GaAs.

The approach described here could prove useful for similar systems. However, we believe that a reason for the success of our approach is that, with the exception of the largest nitrogen concentration at the largest lattice constant, all of our model systems have a positive bandgap. Previous first-principles calculations for the GaAsN system[8-10] have used high nitrogen concentrations in order to obtain smaller model systems, which are computationally less demanding. At these higher concentrations, the LDA bandgap error is so severe that computed band structures do not have a bandgap. This artificial bandgap collapse leads to unofficially occupations of the electronic states (i.e. conduction-band-like states are occupied, while valence-band-like states are unoccupied), producing a significant error in the electronic charge density. In this regime of strongly negative LDA bandgaps, we are not confident that our simple LDA-based approach to computing the pressure dependence of excited state energies could be applied fruitfully.

A remarkable feature of Fig. 2 is the strongly non-linear dependence of the gap on the pressure. This is in marked contrast to the parent GaAs material and provides additional evidence, beyond the large reduction in the bandgap, that a few percent of nitrogen is producing remarkable changes in the material. In order to understand this nonlinearity, it is necessary to study additional bands above the conduction band. Figure 4 shows the theoretical pressure dependence of the Γ-point energies of several additional bands treated with the same analysis that was used for the conduction band in Fig. 2. Eight energy bands of the sys-

tem are shown, but these fall into five degenerate groups. The figure shows three singlet states (filled circles), a doublet (open squares), and a triplet state (open triangles).

A common origin of nonlinear behavior of energy levels as a function of a parameter (such as pressure) is band repulsion. Band repulsion results from the mixing (hybridization) of bands in the same representation of the crystal symmetry group in such a way that level crossings are replaced with non-intersecting horizontal curves separated by a gap-like region. In Fig. 4, the highest singlet on the left and the triplet on the upper right bend downward due to repulsion from higher energy bands that have been omitted from the figure in order to improve its clarity. Whether the upper two singlets cross or repel at about 80 kbar can not be determined from the limited number of points that we have calculated, but if they repel, the effect is not very strong. We have chosen to show the bands as crossing in order to aid the eye in following their relationship with the doublet and the triplet. These assignments were chosen by comparing our results for various nitrogen concentrations with results for pure GaAs with the appropriately folded Brillouin zone. This comparison also allows useful, but non-rigorous, assignments of the low energy GaAsN bands at the Γ-point to special points of the primitive 2-atom GaAs Brillouin zone that are folded into the Γ-point. For the bands shown in Fig. 4, we propose the following assignments: (1) The bottom singlet corresponds to the Γ-point of the fundamental cell. (2) The second singlet on the left hand side (the third singlet on the right) plus the triplet correspond to a split quartet formed from the 4 L-points (111), (1-1-1), (-11-1}), and (-1-11). (3) The remaining singlet plus the doublet correspond to a split triplet consisting of the three X-points (100), (010), and (001). In regions of band repulsion, for example, the character of different bands becomes mixed, and thus these assignments should not be taken too literally. However, we feel that they provide useful labels and help in interpreting the data.

With one exception, all of the bands within a few eV of the gap are observed to regain the degeneracies of pure GaAs to within of a few hundredths of an eV by the time our largest cell (0.78% N concentration) is reached. The exception is the L-derived singlet, which remains split off from the triplet by about 0.1 eV. This suggests that this singlet may evolve into the impurity state observed at very low nitrogen concentrations.[28,29] However, as mentioned above, this state does not act like an impurity state at the technologically interesting concentrations around 2%. Furthermore, the L-derived singlet rises faster than the conduction band throughout the studied pressure range, and we do not see the upward curvature that would be expected if it was repelled by the conduction band. Therefore, we believe that repulsion between the L-derived singlet and the conduction band contributes at most a small amount to the nonlinearity of the conduction band. In contrast, Fig. 4 demonstrates almost textbook repulsion between the X-derived singlet and the conduction band at pressures over 100 kbar, and it is likely that this repulsion continues to lower pressures, even though the effect is obscured by the additional repulsion between the X-derived singlet and a higher state. Based on these observations, we propose that repulsion from the X-derived singlet is the chief cause of the experimentally observed nonlinear dependence of the bandgap on pressure. Based on the above, we conclude that the nonlinear dependence of the bandgap on pressure does not result from localized nitrogen states. Finally, we note that our results are consistent with recent reflectance measurements which show some of the predicted higher energy states.[31,32]

3.2 Conduction-band mass for InGaAsN alloys

There are three convenient methods of using optical measurements for masses, and they are: (1) Study the change in luminescence energy in quantum well structures as a function of the quantum-well width. (2) Measure the quantum well energies by photoreflectance measurements as a function of quantum-well width. (3) Measure exciton diamagnetic shifts as a function of magnetic field. A fourth experimental method, low-temperature measurement of far-infrared cyclotron resonance from n-

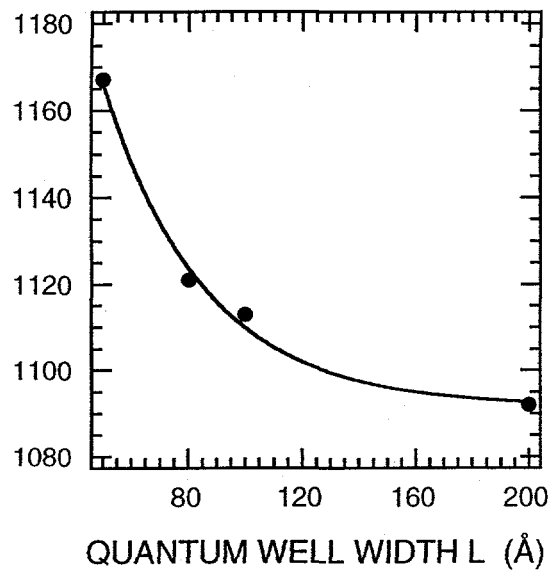

Figure 5. Luminescence energy versus quantum well width L for InGaAsN/GaAs single quantum wells at 4K. The smooth curve drawn through the data is provided an aid to the eye.

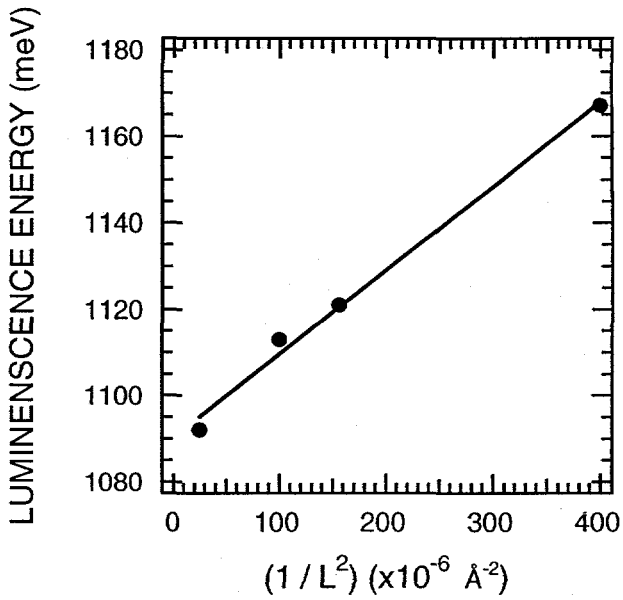

Figure 6. Luminescence energy versus the square of the inverse quantum well width, i.e., L^{-2} for InGaAsN/GaAs single quantum wells at 4K. The straight line fitted to the data. yields an estimate for the conduction-band effective mass $m_c \sim 0.2$.

type samples was attempted, but because of the low transport mobility (~400 cm^2/V-sec), we not able to observe any cyclotron resonance. However, the question regarding the effect of on the conduction-band mass, if any, from adding a small amount of nitrogen to GaAs will now be addressed.

A series of nominally 2% nitrogen InGaAsN/GaAs quantum wells were grown as previously described in Sec. 2. The PL measurements were made at 4K and the resulting dependence of the bandgap energy on the quantum-well width is shown in Fig. 5. The quantum well widths varied between 50 and 200 Å, and as can be seen in Fig. 5, the luminescence energy increases with decreasing quantum well width, the anticipated result. We are interested in comparing the InGaAsN and GaAs masses and thus for purposes of this paper, we will analyze the quantum well data in a simple mannerly assuming infinite barrier heights. Because all of the mass measurements, presented here are only to serve as an illustration of the effect of nitrogen in GaAs, we feel that these simple assumptions are warranted. With the infinite barrier approximation, the luminescence energy is given by

$$E(n) = \frac{\pi^2 \hbar^2 n^2}{2ma^2} = \frac{37600}{m^* L^2}, \text{ (L in Å)}, \tag{1}$$

where n = 1, 2, ... is the quantum number of the state, m^* is the conduction-band effective mass, and L is the quantum well width. Also assumed here is that the InGaAsN/GaAs quantum-well valence-band effective mass is much heavier than the conduction-band mass, and hence the conduction-band mass and not the reduced mass as expressed in Eq. 1. Because the valence-band offset between 2% nitrogen in InGaAsN and GaAs is believed to be small and only due to the offset from the 7% indium content,[3,4] it is reasonable to assume that quantum confinement has not caused a large splitting between the "pinned" heavy-hole and light-hole valence bands, thereby leading to a "heavy" valence-band mass. Figure 6 shows the dependence of the luminescence energy as a function of L^{-2} for the data shown in Fig. 5, and as can be seen, a straight line can be drawn through

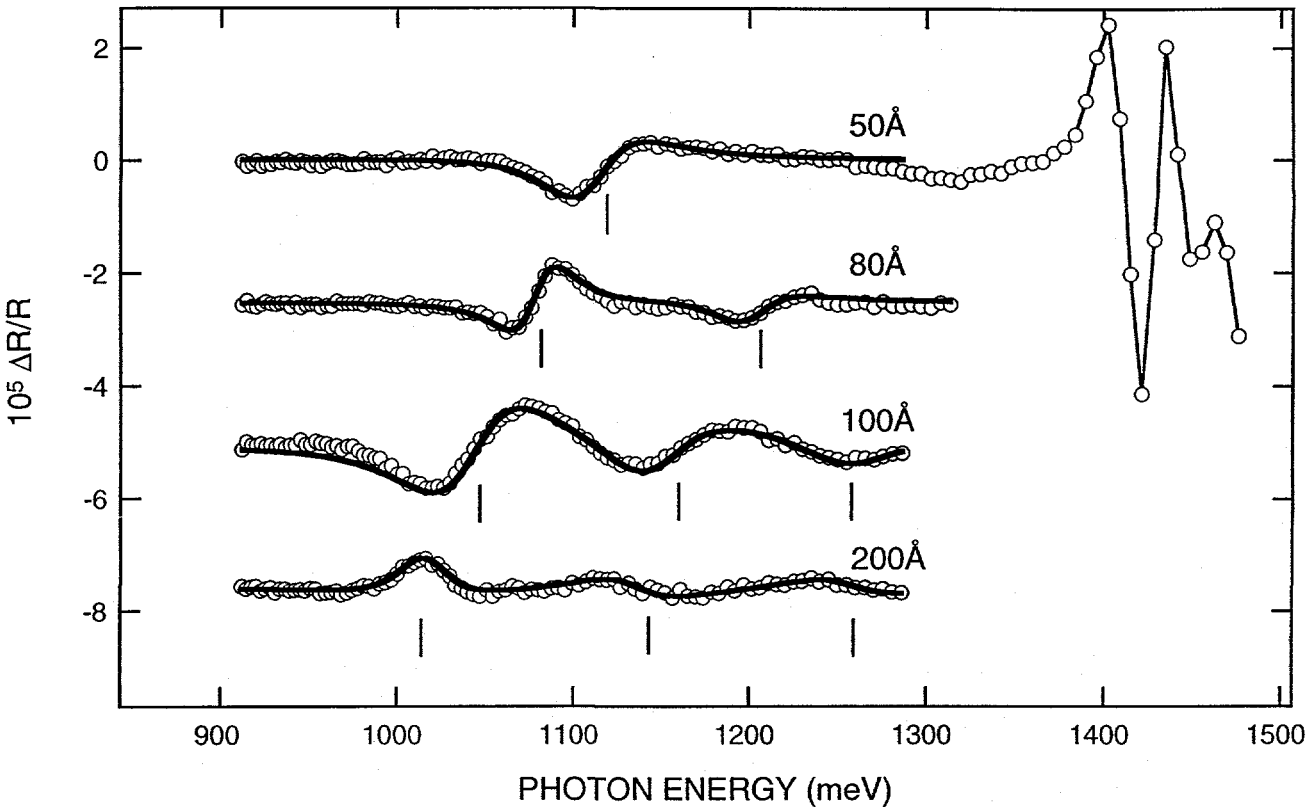

Figure 8. Photoreflectance spectra for four InGaAsN/GaAs quantum well structures. The quantum-well widths are indicated in the figure. The solid lines are "fitted" theoretical photoreflectance line shapes to the data. The vertical lines are the critical point energies (i.e., quantum well energies) for each spectrum as calculated by the theoretical line shape fit. As an aid to the eye, the spectra have been offset from each other.

the data. From the slope of the line shown in Fig. 6 and with n = 1 in Eq. 1, we derive $m_c \sim 0.2$. Possible sources of error in this analysis are the experimental quantum-well widths which are difficult to monitor or control during growth. However, the conduction-band effective mass for GaAs is 0.067 and thus, as in the case of the bandgap energy, we see that the addition of a small amount of nitrogen to GaAs has caused large changes to the 2% nitrogen InGaAsN conduction-band mass.

As mentioned earlier, we have also performed room temperature photoreflectance measurements on the similar structures to those used for the luminescence energy versus quantum-well-width studies. Figure 8 shows photoreflectance spectra for 50, 80, 100 and 200-Å-wide quantum wells. The solid lines are "fitted" theoretical photoreflectance line shapes to the data. The vertical lines are the critical point energies (i.e., quantum well energies) for each spectrum as calculated by the theoretical line shape fit. The difference energy δE from the quantum well states shown in Fig 8 as the vertical lines gives $\delta E \sim 120$ meV. We again make the assumption that this energy difference is due entirely to the conduction-band states. With infinite barrier heights, we can arrive at a qualitative estimate for the conduction-band mass from Eq. 1, with the result $m_c \sim 0.14$, a mass twice as large as that found for GaAs! However, the two measurements of mass are in reasonable agreement with each other and both lead to the conclusion that the conduction-band mass in InGaAsN is two to three times heavier than found for GaAs.

The last experimental method for an optical determination of the conduction-band mass involves measurements of the exciton diamagnetic shift as a function of magnetic field for 2% nitrogen InGaAsN alloys lattice matched to GaAs. The mag-

netoexciton diamagnetic shift dependence on magnetic field for ambient pressure is shown as closed circles in Fig. 8. The diamagnetic shifts for varying InGaAsN conduction-band mass between $m_c = 0.067$ and 0.5 are also indicated in the figure. The theoretical diamagnetic shifts were calculated by the variational approach as described by Greene and Bajaj.[33,34] For the diamagnetic shift calculation presented here, we adapted our quantum-well computer codes[35] which were used to quantify the diamagnetic shift studies in (411)A-oriented GaAs/AlGaAs quantum wells. We account for the 3D (bulk) excitons in InGaAsN by setting the InGaAsN quantum-well width to 2000Å. The trial wavefunctions are expressed in terms of a Gaussian basis set with the magnetic field perpendicular to the growth direction, i.e., the exciton orbits are in the plane of a 2000-Å-wide InGaAsN/GaAs quantum well. The exciton binding energies are calculated for finite values of the height of the 7% indium InGaAsN-GaAs potential barrier. The envelope function method is also employed to account for the finite quantum-well width and height. Besides the low temperature bulk GaAs bandgap energy, the magnetic field strength, and the quantum-well width, some of the relevant physical parameters include: (1) Conduction and valence-band offsets between InGaAsN quantum well and the GaAs barriers. (2) The Luttinger parameters γ_1 and γ_2 for both the InGaAsN quantum well and GaAs barriers. (3) Conduction and valence-band mass values for the InGaAsN quantum well and GaAs barrier. (4) Low frequency dielectric constants ε_0 for the quantum well and barrier materials. For these calculations, GaAs values for all parameters except the conduction-band mass were used not only for the GaAs barrier, but also for the InGaAsN quantum well. For the present stage of understanding the electronic properties of InGaAsN alloys, these assumptions are reasonable. As can be seen in Fig. 8, a best fit diamagnetic shift dependence on magnetic field occurs for an InGaAsN conduction-band effective mass $m_c \approx 0.13$, which is in excellent agreement with the two previous optical determinations presented in this paper of the energy versus quantum-well width studies which gave $m_c = 0.2$ and the analysis of the quantum-well states of the photoreflectance data which yielded $m_c = 0.13$.

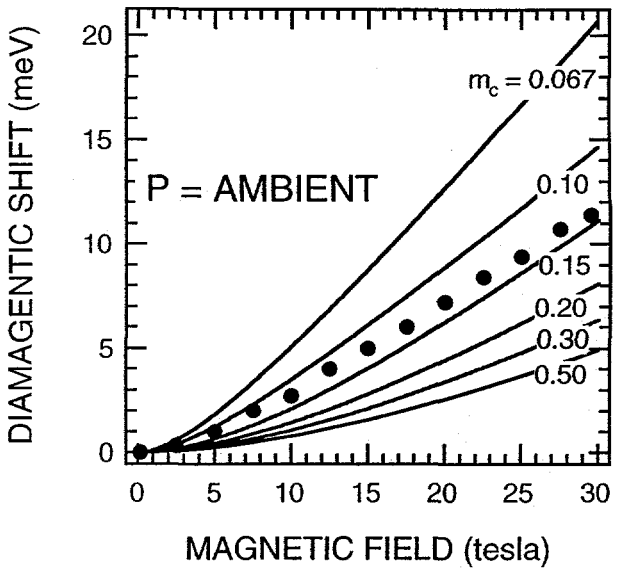

Figure 8. Ambient-pressure exciton diamagnetic shift as a function of magnetic field at 2K for 2% nitrogen InGaAsN alloy. The closed circles are the experimental points. The curves, labeled $m_c = 0.067$ to 0.50, are calculated diamagnetic shifts as a function of mass. The estimated ambient pressure InGaAsN conduction-band effective mass m_c is about 0.13.

3.3 Pressure dependence of the InGaAsN conduction-band effective mass

As mentioned in the experimental section, pressure dependent magnetoluminescence measurements were performed in the pressure range of ambient to 110 kbar and magnetic fields up to 30 tesla. The diamagnetic shift data can be readily analyzed for pressures less than 40 kbar. For higher pressures, the accuracy of the technique fails because of linewidth broadening by the non-hydrostatic component of the pressure medium and also because of an large increase of the conduction-band mass as discussed below.

Figure 9 shows the magnetic field dependence of the exciton diamagnetic shift at 38 kbar and T = 2K. As is the case with Fig 8, the filled circles are the data points and the curves are calculated shifts as a function of mass. It is apparent from the figure that the conduction-band effective mass is nearly 0.2 in contrast to the $m_c = 0.13$ found from the ambient pressure data.

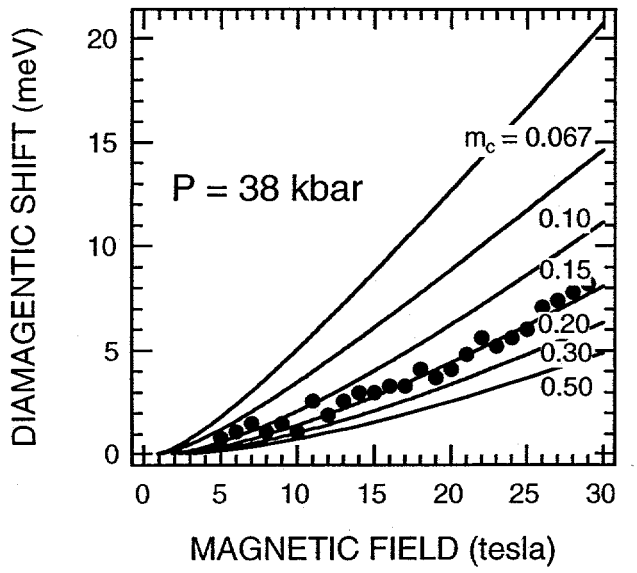

Figure 9. Exciton diamagnetic shift as a function of magnetic field and 38 kbar at 2K for the 2% nitrogen InGaAsN alloy. The closed circles are the experimental points. The curves, m_c = 0.067 to 0.50, are theoretical diamagnetic shifts as a function of mass. The estimated InGaAsN conduction-band effective mass at 38 kbar is $m_c \approx 0.2$.

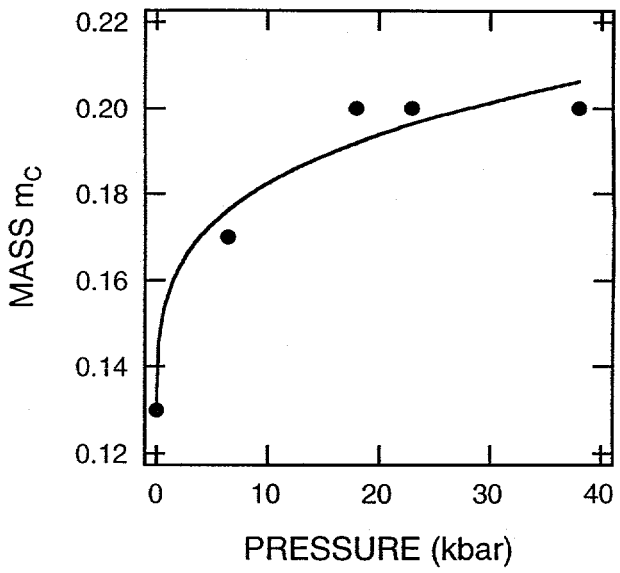

Figure 10. The 2-K pressure dependence of the conduction-band mass between ambient pressure and 40 kbar for the 2% nitrogen InGaAsN sample. The smooth curve drawn through the data provides an aid to the eye.

This large increase to the mass for 2% nitrogen in GaAs is surprising. Recently, we have reported[36] mass measurements as a function of pressure in $In_{0.2}Ga_{0.8}As/GaAs$ strained-single-quantum wells and, found that the conduction-band mass ranged from ~0.07 to ~0.085 for pressures between ambient and 36 kbar in a linear manner. This result for InGaAs/GaAs agrees with expectations based on simple ***k•p*** theory.[36] The large variation and nonlinear behavior of the conduction-band mass for InGaAsN may not be that surprising in light of all of the other mysteries associated with substituting nitrogen for arsenic in GaAs. Figure 10 shows the variation of the effective mass for pressures between ambient and 38 kbar. The smooth curve provides an aid to the eye.

Because of our success in using the LDA calculation to quantify the change in the bandgap energy with pressure (Fig. 2), we performed preliminary LDA calculations for the pressure dependence of the conduction-band mass. But to date, our results are inconclusive and are not ready to be discussed here. We can, however, make some qualitative statements by examining the LDA results shown in Fig. 4. As discussed earlier, the band repulsion between the Γ-like and X-like bands at high pressure indicate that strong Γ-X mixing is occurring. Because the mass of the six-fold degenerate X-point in GaAs is heavy (m_{Xt} = 1.2 & m_{Xl} = 0.27), we expect that the Γ-X mixing will cause a corresponding increase to the Γ-like conduction-band mass by the heavy X-like mass. Part of the LDA mass calculation will require information about the X-like as well as the L-like masses. In the future, an obvious goal of our LDA calculations will be to replicate the curve shown in Fig. 10.

4. CONCLUSIONS

We have shown that while the first principles LDA calculation for the band structure of InGaAsN yields incorrect values for the bandgap energy, the predicted change in bandgap energy with pressure is in excellent agreement with experiment. Both experiment and calculations show that the lack of crossing of the Γ-like and X-like conduction bands is due to Γ-X mixing. The conduction-band effective mass was measured by three techniques with the result for 2% InGaAsN, lattice matched to GaAs, the ambient pressure conduction-band effective mass $m_e \approx 0.13$. The pressure dependence of the conduction-band mass is nonlinear and large. The current challenge of the LDA calculation is to account for this behavior.

ACKNOWLEDGEMENTS

The authors wish to thank Dr. Yong-Jie Wang of the National High Magnetic Field Laboratory for the far-infrared cyclotron measurements, Dr. D. M. Follstaedt and Dr. Charles Barbour of Sandia National Laboratories for providing the results of their transmission electron microscopy measurements and elastic recoil detection measurements. Sandia is a multiprogram laboratory operated by Sandia Corporation, a Lockheed Martin Company, for the United States Department of Energy under contract DE-AC04-94AL85000. Part of this work was performed at the National High Magnetic Field Laboratory, which is supported by NSF Cooperative Agreement No. DMR-9016241 and by the State of Florida, and by a grant of HPC time from the DoD HPC ARL and CEWES Major Shared Resource Centers. The *ab initio* total-energy and molecular-dynamics package VASP (Vienna *Ab initio* Simulation Package) and the corresponding ultrasoft pseudopotential database were developed at the Institute für Theoretische Physik of the Technische Universät Wien.

REFERENCES

1. W. G. Bi and C. W. Tu, "Bowing parameter of the band-gap energy of GaN_xAs_{1-x}," Appl. Phys. Lett. **70**, pp. 1608-1610, 1997.
2. L. Malikova, F. H. Pollak, and R. Bhat, Composition and temperature dependence of the direct band gap of $GaAs_{1-x}N_x$ ($0 \le x \le 0.0232$) using contactless electroreflectance," J. Electronic Materials **27**, pp. 484-487, 1998.
3. M. Kondow, K. Uomi, A. Niwa, T. Kitatani, S. Watahiki, and Y. Yazawa, "GaInNAs: A novel material for long-wavelength-range laser diodes with excellent high-temperature performance," Jpn. J. Appl. Phys. **35**, pp. 1273-1275, 1996.
4. M. Kondow, T. Kitatani, S. Nakatsuka, M. C. Larson, K. Nakahara, Y. Yazawa, M. Okai, and K. Uomi, "GaInNAs: A novel material for long wavelength semiconductor lasers," IEEE J. Selected Topics in Quantum Electronics **3**, pp. 719-729, 1997.
5. T. Miyamoto, K. Takeuchi, F. Koyama, and K. Iga, "A novel GaInNAs-GaAs quantum-well structure for long-wavelength semiconductor lasers,", IEEE Photonics Tech. Lett. **9**, pp. 1448-1450, 1997.
6. Sarah R. Kurtz, D. Myers, and J. M. Olsen, "Projected Performance of Three- and Four Junction Devices Using GaAs and GaInP", in *Proc. 26th IEEE Photovoltaics Spec. Conf.* (IEEE, New York, 1997) pp. 875-878.
7. Steven R. Kurtz, A. A. Allerman, E. D. Jones, J. M. Gee, J. J. Banas, and B. E. Hammons, "InGaAsN solar cells with 1 eV bandgap, lattice matched to GaAs," To be published, Appl. Phys. Lett.
8. A. Rubio and M. L. Cohen, "Quasi-particle excitations in $GaAs_{1-x}N_x$ and $AlAs_{1-x}N_x$ ordered alloys," Phys. Rev. B **51**, pp. 4343-4346, 1995.
9. J. Neugebauer and C. G. Van de Walle, "Electronic-structure and phase-stability OF $GaAs_{1-x}N_x$ alloys," Phys. Rev. B **51**, pp. 10568-10571, 1995.
10. S.-H. Wei and A. Zunger, "Giant and composition-dependent optical bowing coefficient in GaAsN alloys," Phys. Rev. Lett. **76**, pp. 664-667, 1996.
11. L. Bellaiche, S.-H. Wei, and A. Zunger, "Localization and percolation in semiconductor alloys," Phys. Rev. B **54**, pp. 17568-17576, 1996.
12. L. Bellaiche, S.-H. Wei, and A. Zunger, "Band gaps of GaPN and GaAsN alloys," Appl. Phys. Lett. **70**, pp. 3558-3560, 1997.
13. L. Bellaiche, S.-H. Wei, and A. Zunger, "Composition dependence of interband transition intensities in GaPN, GaAsN, and GaPAs alloys," Phys. Rev. B **56**, pp. 10233-10240, 1997.

14. L. Bellaiche and A. Zunger, "Effects of atomic short-range order on the electronic and optical properties of GaAsN, GaInN, and GaInAs alloys," Phys. Rev. B **57**, pp. 4425-4431, 1998.
15. E. D. Jones, N. A. Modine, A. A. Allerman, S. R. Kurtz, A.F. Wright, S. T. Tozer, and X. Wei, "Band structure of InGaAsN alloys and effects of pressure," submitted to Phys. Rev. Lett. (1999).
16. X. Zhu, S. Fahey, and S. G. Louie, "*Ab initio* calculation of pressure coefficients of band gaps of silicon: Comparison of local-density approximation and quasiparticle results," Phys. Rev. B **39**, pp. 7840-7847, 1989.
17. E. V. K. Rao, A. Ougazzaden, Y. Le Bellego, and M. Juhel, "Optical properties of low band gap $GaAs_{(1-x)}N_x$ layers: Influence of post-growth treatments," Appl. Phys. Lett. **72**, pp. 1409-1411, 1998.
18. D. M. Follstaedt (Unpublished results).
19. S.W. Tozer (Unpublished results).
20. G. J. Piermarini, S. Block, J. D. Barnett, "Hydrostatic limits in liquids and solids to 100 kbar," J. Appl. Phys. **44**, pp. 5377-5382, 1973.
21. R. A. Forman, G. J. Piermarini, J. D. Barnett, S. Block, "Pressure measurement made by the utilization of ruby sharp-line luminescence," Science **176**, pp. 284-285, 1972.
22. See for example E. D. Jones, S. T. Tozer, and T. Schmiedel, "Pressure dependence of the bandgap energy and the conduction-band mass for an n-type InGaAs/GaAs single-strained quantum well, Physica E **2**, pp. 146-150, 1997.
23. G. Kresse and J. Hafner, "*Ab initio* molecular-dynamics for liquid-metals," Phys. Rev. B **47**, pp. 558-561, 1993.
24. G. Kresse and J. Hafner, "*Ab-initio* molecular-dynamics simulation of the liquid-metal amorphous-semiconductor transition in germanium," Phys. Rev. B **49**, pp. 14251-14269, 1994.
25. G. Kresse and J. Furthmüller, "Efficiency of *ab-initio* total-energy calculations for metals and semiconductors using a plane-wave basis-set," Comput. Mat. Sci. **6**, pp. 15-50, 1996.
26. G. Kresse and J. Furthmüller, "Efficient iterative schemes for *ab-initio* total-energy calculations using a plane-wave basis-set," Phys. Rev. B **54**, pp. 11169-11186, 1996.
27. D. Vanderbilt, "Soft self-consistent pseudopotentials in a generalized eigenvalue formalism," Phys. Rev. B **41**, pp. 7892-7895, 1990.
28. V. Fiorentini, M. Methfessel, and M. Scheffler, "Electronic and structural-properties of GaN by the full-potential linear muffin-tin orbitals method: The role of the d-electrons," Phys. Rev. B **47**, pp. 13353-13362, 1993.
29. D. J. Wolford, J. A. Bradley, K. Fry, and J. Thompson, "The nitrogen isoelectronic traps in GaAs," in *Physics of Semiconductors*, ed. J. D. Chadi and W. A. Harrison (Springer, New York, 1984) pp. 627-630.
30. X. Liu, M. E. Pistol, L. Samuelson, S. Schwetlick, and W. Seifert, "Nitrogen pair luminescence in GaAs," Appl. Phys. Lett. **56**, pp. 1451-1453, 1990.
31. J. D. Perkins, A. Mascarenhas, Y. Zhang, J. F. Geisz, D. J. Friedman, J. M. Olson, and S. R. Kurtz, "Direct observation of resonant-level-induced giant bowing in $GaAs_{1-x}N_{x,,}$" To be published Phys. Rev. Lett., 1999
32. W. Shan, W. Walukiewicz, and J. W. Ager III, "Band anticrossing in GaInNAs alloys," To be published Phys. Rev Lett., 1999.
33. R. L. Greene and K. K. Bajaj, "Effect of a magnetic field on the energy levels of a hydrogenic impurity center in GaAs/$Ga_{1-x}Al_xAs$ quantum-well structures,", Phys. Rev. B **31**, pp. 913 - 918, 1985.
34. R. L. Greene and K. K. Bajaj, "Binding energies of Wannier excitons in GaAs-$Ga_{1-x}Al_xAs$ quantum-well structures in a magnetic field,", Phys. Rev. B **31**, pp. 6498 - 6502, 1985.
35. E. D. Jones, K. Shinohara, S. Shimomura, S. Hiyamizu, I. Krivorotov, and K. K. Bajaj, "Magneto-excitons in (411)A and (100)-oriented GaAs/AlGaAs multiple quantum well structures," in *Physics and Simulation of Optoelectronic Devices VII,* edited by M. Osinski, P. Blood, and A. Ishibashi, SPIE Conference Proceedings Vol. **3625** (International Society for Optical Engineering, Bellingham, WA, 1999).
36. E. D. Jones, S. T. Tozer, and T. Schmiedel, "Pressure Dependence of the Bandgap Energy and the Conduction-Band Mass for an n-type InGaAs/GaAs Single-Strained Quantum Well," Physica E **2**, pp. 146-150, 1998.